**Ethiopian Journal of Water Science and Technology (EJWST)**

**DOI:** https://doi.org/10.59122/17519t6

Vol. 7 , 2024, pages: 1~19 ISSN(Print): 2220-7643

# Remote Sensing Approach for Detection and Attribution of Flood Inundation, Lower Awash Basin, Ethiopia

**Tilaye Worku Bekele [b*], Ephrem Derso Negash [b], Wegayehu Asfaw[b,c], Alemseged Tamiru Haile[a]**

[a]*International Water Management Institute (IWMI), P.O.Box, 5689, Addis Ababa, Ethiopia.; [b]Water Technology Institute, Arba Minch University, P.O. Box 21, Arba Minch, Ethiopia; [c]Department of Water Resources, Faculty of Geo-Information Science and Earth Observation (ITC), University of Twente, 7522 NH, Enschede, the Netherlands*.

[*]Corresponding author: Email: tworkcon@gmail.com, P.O. Box: 21, Arba Minch University, Arba Minch, Ethiopia.

**Abstract**

Flood risk management has been severely constrained by limited information on the causes and impacts of flooding. In this study, we evaluated the effect of short-term land cover change of Logiya Catchment on flood inundation to impact Dubti town and its surroundings in the Lower Awash Basin, Ethiopia. We used Sentinel-1 Synthetic Aperture Radar (S-1 SAR) data to detect flood but Sentinel-2 (S-2) optical satellite data to classify land cover by applying a machine learning algorithm. We also used land cover and soil data to generate the Curve Number (CN) map of the study area from 2017 to 2023. The flood maps showed that roads and irrigation canals were washed away by the 2020 extreme flood, which led to the inundation and abandonment of the Tendaho Irrigation Scheme. The runoff generation potential (CN) was above 27% at the Logiya Catchment from 2017 to 2023, contributing to severe flooding. The remote sensing analysis showed that overflow of the Logiya River in 2020 was intercepted and conveyed by the main irrigation canal of the Tendaho Scheme resulting in inundation of the Dubti and its surroundings. The flood extent at Dubti and its surroundings was 59.22 $km^2$ in 2020. It increased by 26% from 2017 to 2019. Frequent (6-days), high resolution (10m) and time-series 7 years Sentinel-1 data helped to get a detailed characterization of the cause, dynamics, and impacts of the historical flood events. The approach and results of this study can guide flood risk management in the study area and serve as a reference for future studies in other flood affected areas.

**Keywords**: Sentine-1 SAR, flood mapping, land cover, attribution, Awash-Basin, Logiya catchment, Dubti town.

Date received: 7 Oct. 2024; Received in the revised form : 22 Feb 2024; Accepted: 30 November . 2024; Published: December , 2024

## 1. INTRODUCTION

In Ethiopia, flooding is a major natural hazard that hinders economic development and causes loss of human life (Tamiru & Dinka 2021; Bibi et al. 2023). In 2016, flood damaged households (6249 USD) and farmland (5326 USD) in central rift-valley basin (Edamo et al. 2022). Major cities of the country such as Addis Ababa, Adama, and Dire Dawa are under flood risk. Specifically, 25 % of Adama city is vulnerable to flooding (Leta & Adugna 2023) and 44,544 and 77,320 buildings in Addis Ababa are exposed to floods of 1-in-5 and 1-in-100 years return, respectively (Carr et al. 2024; Asfaw et al. 2025). The flood risk of these cities can be associated with low coping capacity (Erena & Worku 2019) and bio-physical factors. Hence, flood studies are essential to enhance the coping and adaptation capacities of the cities and towns of Ethiopia (Haile et al. 2024).

Stream-flow monitoring in Ethiopia is hampered by the decline of ground-based monitoring stations that often do not cover flood prone areas (Haile et al 2022). As a result, flood risk management is commonly based on limited data and knowledge about past floods. Earth observation satellite can fill such data gap by monitoring during both day and night as well as in all weather conditions (Li et al. 2018). Optical remote sensing satellites incapable monitor floods during cloudy seasons (Munasinghe et al. 2023; Matheswaran et al. 2019). The S-1 SAR provides images at 10 meter horizontal spatial resolution every 12 or 6-day intervals subject to geographic locations (Mohammadi et al. 2020). However, the S-1 data requires pre-processing to minimize the effects of buildings, vegetation (Nuthammachot et al. 2017), and topography (Zeng et al. 2020) on the imagery.

Low signal backscatter intensity of S-1 SAR indicates flooded surface. This can be distinguished from non-flooded surface by histogram thresholding (Cao et al. 2019) and/or change detection (Clement et al. 2017). The accuracy of these methods can be enhanced using ground based reference data (e.g. Bekele et al. 2022). Obtaining such data may not be easy owing to the limitation of existing ground-based measurement equipment. As a result, proxy data is often used to calibrate or validate flood maps while some researchers use secondary data as ground-based reference data. Using the flood data from the S-2 optical imagery as a reference, Kianfar (2019) reported 68% accuracy in the flood map generated using the S-1 SAR data. Using field surveyed data and flood maps generated by the community as a reference, Haile et al (2023) reported 95% accuracy of the flood map detected from S-1 SAR data.

Flood can be intensified owing to changes in the runoff generation potential (Curve Number) of the upstream catchments. The Curve Number (CN) can serve as a proxy to estimate the surface runoff generating potential based on the land use and soil characteristics of the catchment (Prabhu et al. 2020). Changes in CN can be caused by urbanization (Miller et al. 2014), deforestation, agricultural practices and ecological transformations (Fang et al. 2022). Hence, time series land cover classification enables monitoring of changes in CN across a catchment. Machine learning (ML) algorithms are receiving popular applications for land cover classifications (Dash et al. 2023). However, these algorithms remain confusing while classifying the built-up and sandy areas, and irrigated and shrub land cover classes (Thakkar et al. 2017). However, classification accuracy of shrub and pasture land can be improved using remote sensing indices (e.g. Normalized Difference Vegetation Index, NDVI) to train Machine Learning (ML) algorithm. Manandhar et al (2009) applying a rule (knowledge based logic) to differentiate built-up area from vegetation land increased the land cover accuracy from 70 to 90%. Dash et al (2023) detected the water body using Normalized Difference Water Index (NDWI) and manually digitized the sandy area following the drainage network of the catchment. Thus, sandy area was excluded from training the ML algorithm to reduce the commission error in built-up and overlaid to enhance the overall accuracy of land cover from 67 to 82 %. These studies indicated that post-classification can enhance the accuracy of land cover classification using ML methods.

This study examines the interaction between flood and land cover in the flood-prone area of Lower Awash Basin, Dubti, Ethiopia. It uses the CN difference between 2017 and 2023 to assess the effect of temporal variability of land cover on the flood generation potential of the Logiya Catchment. The study also examines the inter-annual variability of flood extent and impact in the surrounding of Dubti town.

## 2. Description of the Study Area

Logiya is an upland catchment that drains from the northern upstream parts of the Awash Basin in Ethiopia. Geographically, the catchment is located between 39.5$^{o}$ to 41.0$^{o}$ E and 12.1$^{o}$ to 11.6$^{o}$ N. The Logiya River joins the Awash River just downstream of the Logiya Bridge. The catchment covers an area of 4687 $km^2$ and has a high potential to generate significant flooding because of steep terrain slope and sparse vegetation cover while the flood affects the Ethio-Djibouti road between Logiya and Semera town.

The terrain elevation of the catchment varies from a maximum of 3602 m to 376 m a.m.s.l. Moderate slopes (5 to 10 %) cover 24 % of the catchment. The steep and extremely steep slopes (> 15 %) that generate rapid surface runoff cover 14 % of the catchment.

The Logiya Catchment is dominantly covered with farmland, mixed forest, shrub, and bare-land. The eastern upstream part of the catchment is dominantly farmland, while the middle to downstream parts are dominantly bare-land and shrubs. Based on the runoff generation potential, the soil of the catchment is categorized into three hydrological soil groups: A, B, and D. Hydrological soil group D, with high runoff potential covers 76% of the catchment while hydrological soil group A and B cover 5 and 19 %, respectively.

Dubti, situated at the downstream part of Awash Basin, has a population density of 20.6/$km^2$ [1]. The main irrigation canal of the Tendaho Irrigation Development Project conveys water through the town to irrigate the surrounding agricultural lands. (Figure 1 (d).

The climate of the lower Awash Basin is divided into three seasons: dry season (Bega) from October to February, short rainy season (Belg) from March to June, and wet season (Kiremt) from July to September (Malede et al. 2024; Taye et al. 2018 and Haile et al. 2023).

[1] https://www.citypopulation.de/en/ethiopia/admin/afar/ET020101__dubti/

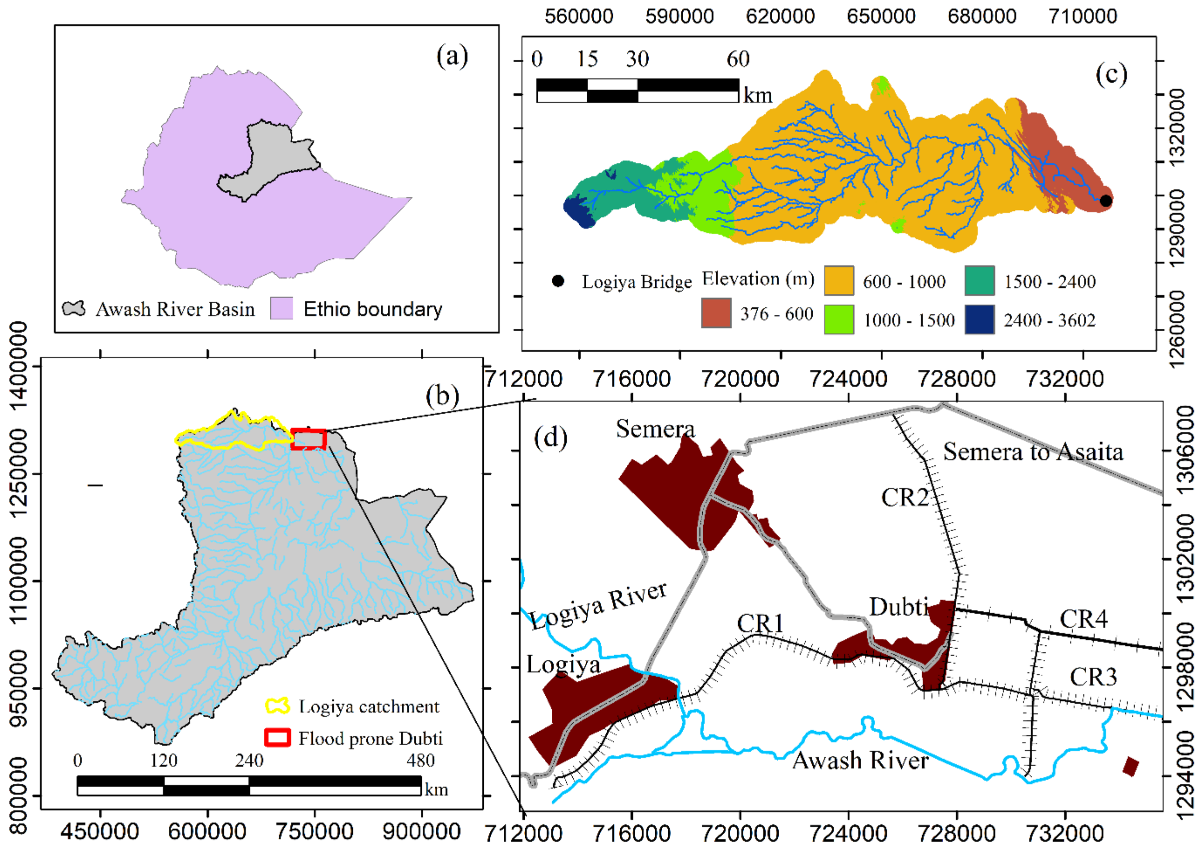


Figure 1. Location map of the study area, (a) location of Awash Basin in the Ethiopia, (b) the Logiya Catchment (yellow polygon) and flood prone area of Dubti (red rectangle), (c) the elevation map of Logiya Catchment and (d) Dubti and other nearby towns. CR represents main canal with access road stretching along the canal and numbers indicate the various canals

## 3. Materials and Methods

### 3.1. Materials

The data inputs of this study were Ground Control Points (GCPs) collected from the field and Google Earth images; community consultation (to select the study site of Logiya Catchment and historical flood extent delineation) (Haile et al. 2023); satellite images (S-1 SAR and Sentinel-2); and global datasets (250m resolution soil data and elevation data)[2]. As there was no registered flood parameter data, the researchers consulted with the community to identify the maximum flood extent that occurred in 2020. Thus, the flood extent map generated by the community was used to train and validate the remote sensing index used for flood monitoring.

[2] https://www.isric.org/explore/isric-soil-data-hub

The Digital Elevation Model (DEM) of 30m horizontal spatial resolution from Shuttle Radar Topography Mission (STRM) was used to reduce the shadow effect in flood mapping using S-1 SAR. S-2 was used to detect the land use and land cover.

The land cover map was detected using a Classification and Regression Tree (CART) machine learning algorithm. It performed better than other machine learning algorithms existed in Google Earth Engine (GEE) cloud computing platform for land cover classification in upper Awash Basin (Negash et al. 2023; Bekele et al. 2022). We used a Root of Normalized Image Difference method selected by Haile et al (2023) for flood detection using S-1 SAR images at the Awash Basin from 2017 to 2022. However, in this study, flood map was extended to 2023 so as to identify new flood-affected area and associated impact.

### 3.2. Methods

Pre-processed S-2 and S-1 satellite imageries were used to generate multi-temporal land cover and flood maps respectively in the GEE platform (Gorelick et al. 2017). The S-2 dataset was filtered using cloud probability pixels and Air Quality band (Q60) to obtain cloud-free images. The Ground Range Detection format of the S-1 SAR, with VH polarization undergoing radiometric and geometric correction, was employed for flood monitoring. However, the speckle noise of S-1 imageries was filtered using a 3x3 median filtering approach widely used for flood monitoring (Kianfar 2019; Anusha & Bharathi 2020) . To reduce the shadow effect, the S-1 SAR images were laid to mask the terrain with a slope above 2%. In this study, the start of the analysis period was 2017 considering the joint availability of S-1 SAR and S2 satellite images.

### 3.3. Land Cover mapping

GCPs were collected from Google Earth images while field survey was done to train and validate the ML algorithm of land cover mapping. During the field survey (14 to 18 July 2023) at Dubti flood-prone area, six major land cover classes were identified: agricultural land, bare-land, built-up, mixed forest, shrub land, and water body. Thus, 121 GCPs from both homogeneous and mixed land cover classes with land size of at least three-pixel sizes of S-2 (30x30m) image were collected. Then, additional 193 GCPs were collected from Google Earth Satellite image based on knowledge of the study site, and were used to train the ML algorithm. Based on previous research experiences, at least 30 GCPs per each land cover classes should be used to train the ML algorithm during LC classification. These, ground truth data collected during filed visit in 2023 was used to validate the ML algorithm performance in land cover classification by using confusion matrix.

At Logiya Catchment, 214 GCPs were collected from Google earth images guided by Normalized Difference Water Index (NDWI) to distinguish the water body and Normalized Difference Vegetation Index (NDVI) to identify shrub land from bareland in 2023. Similarly, 153 GCPs were collected to classify the 2017 land cover. Then, the 2017 and 2023 land cover maps were used to examine the land cover change effect in the runoff generation potential of the catchment.

### 3.4. Accuracy assessment

In this study, the confusion matrix that contained (n x n) row and column size was constructed. In this case, ‘n’ referred to the number of land cover classes. The matrix showed (number of GCPs collected from different land cover classes during actual field observation) laid under different land cover classes detected from remote sensing. The diagonal element of the matrix indicated the number of correctly classified land cover classes compared with actual field observation. Then, the overall accuracy was determined by the percent of accurately classified land cover (the sum of diagonal elements of the matrix) compared with the total GCPs (Rwanga & Ndambuki 2017).

To determine producer’s accuracy, the number of correctly classified reference GCPs of each land cover class was divided by the total number of reference GCPs laid in a particular land cover class. On the other hand, user’s accuracy was determined when the number of correctly classified reference GCPs was divided by the total number of classified pixels in that class. The omission and/or commission errors are calculated by subtracting the producer’s and user’s accuracy from 100%, respectively.

In post land cover classification, the built-up and irrigated land were masked in re-classifying the land cover map of flood prone area. Thus, used to reduce the commission and omission error reported between built-up and sandy area, and shrub land and irrigated (Manandhar et al. 2009). Therefore, the accuracy of land cover map of 2023 Dubti flood prone area before and after post-processing was determined by reference GCP collected from the field.

### 3.5. Land cover effect on flood generation

The change in runoff generating potential of Logiya Catchment was examined by using the land cover map of 2017 and 2023, and soil data collected from global dataset. The soil data was reclassified with the hydrological soil group of A, B, and D. The reclassified soil data and land cover map were jointly used to estimate the CN, a proxy for runoff generation potential (Prabhu et al. 2020). In this study, the difference in the CN maps of 2017 and 2023 was reclassified into five classes (less than -20, -5 to -20, -5 to 5, 5 to 20, and greater than 20). Negative CN differences represented reduction in runoff generation potential, while differences between -5 and 5 indicated no change in runoff generation. However, pixels with values greater than 5 showed increased potential to generate runoff and contributed to flood generation over the downstream flood-prone sites.

The Root of Normalized Image Difference method was used to extend flood maps from 2017 to 2022, as reported by Haile et al (2023) to 2023. The method performed better in accuracy when validated through flood map generated by participatory mapping involving the community members. Reference is made to Bekele et al (2022) for detail about the RNID flood detection method. This study examined new flood-affected areas and their interaction with local environment, examining floods detected from 2017 to 2019, 2020. Figure 2 showed the workflow diagram of this study.

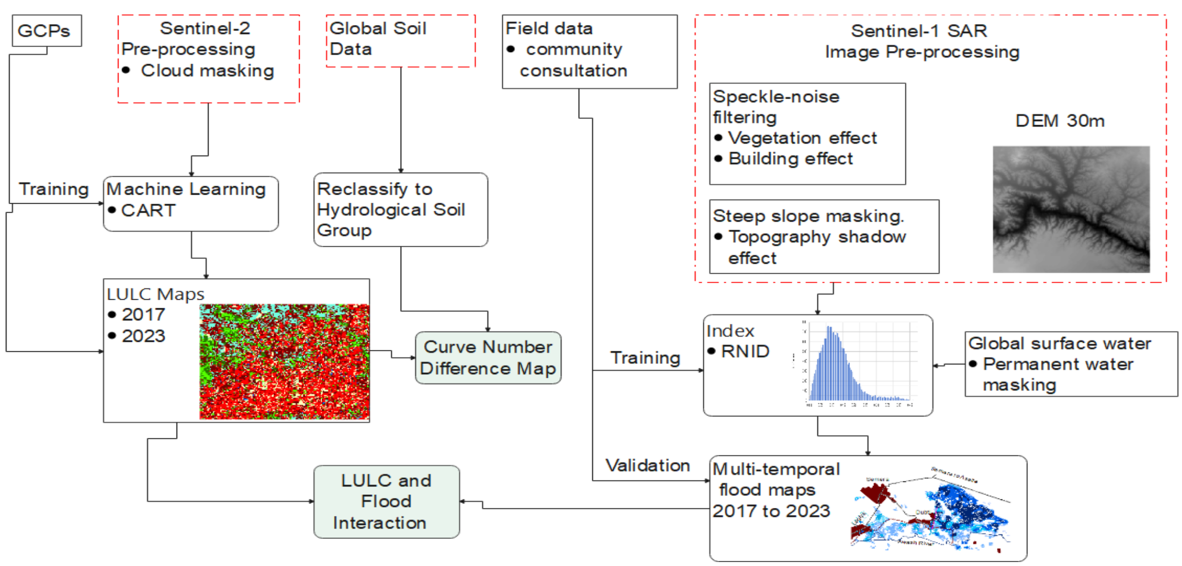


Figure 2. Workflow diagram synthesizing the methods of this study

# 4. Results and Discussion

## 4.1. Land Use classification

In this section, the land use maps of Logiya Catchment, Dubti flood-prone area, classification accuracy, CN difference, and flood maps were presented and interpreted. The 2017 and 2023 land cover maps of Logiya Catchment and Dubti flood-prone area were compared.

In 2017, the middle and lower parts of the Logiya Catchment were dominated by bareland and shrub lands, while disconnected agricultural land dominated the upper part of the catchment (Figure 3a). In 2023, agricultural land concentration increased in the western (upstream) part and expanded in small pockets to the other parts of the catchment, reducing shrub and bareland (Figure 3b). Some disconnected agricultural land were connected, while mixed forest areas increased in the western upstream part.

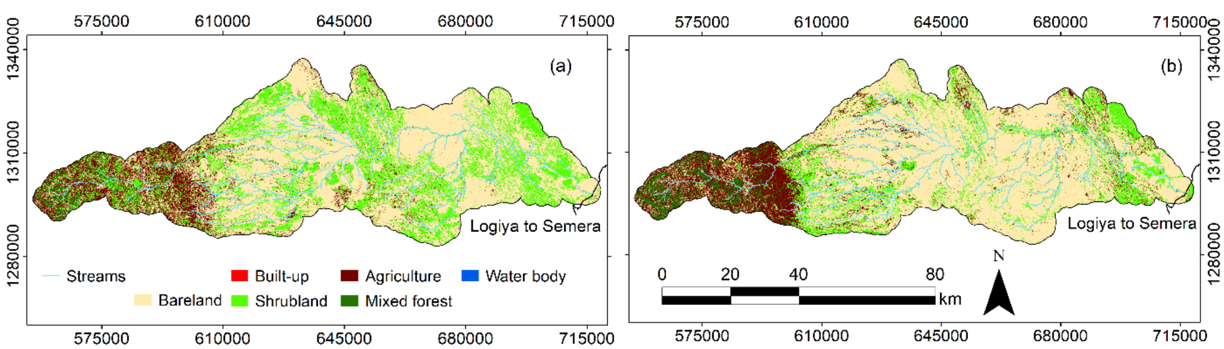


Figure 3. (a) the 2017 LULC map, and (b) the 2023 LULC map of Logiya Catchment

Table 1 showed the percentage of each land cover class of Logiya Catchment in 2017 and 2023. All land cover classes experienced a change within these years. From the perspective of runoff generation, the major changes were expansion of the bareland, farmland and built-up area and reduction of the shrub land. The land cover classes that experienced expansion enhanced runoff generation in the catchment to affect the downstream area. However, the increasing of mixed forest reduced runoff though it increased by more than two-folds in Logiya Catchment.

Table 1. Percentage of each land cover class of Logiya Catchment in 2017 and 2023

| | Percentage of area coverage | |
|---|---|---|
| Land Cover type | 2017 | 2023 |
| Bare land | 59.83 | 66.32 |
| Built-up | 0.02 | 0.22 |
| Shrubland | 27.76 | 16.36 |
| Farmland | 10.89 | 13.24 |
| Mixed forest | 1.47 | 3.81 |

## 4.2. Curve Number Difference and Flood Interaction

Figure 4 showed positive CN differences between 2017 and 2023, slightly surpassing the negative differences suggesting most parts of the catchment experienced increased runoff generation potential. Positive CN differences reported near the catchment outlet had a potential to generate flash floods during intense rainfall conditions. This was in agreement with the opinion of some of the residents in Logiya. They believed that flash floods were common in the area. The positive differences over the upstream part could also be concerning as these areas were characterized by steep slopes that enhanced flood generation potential of the catchment. Most of the middle part of the catchment did not experience a significant change in potential runoff generation between 2017 and 2023.

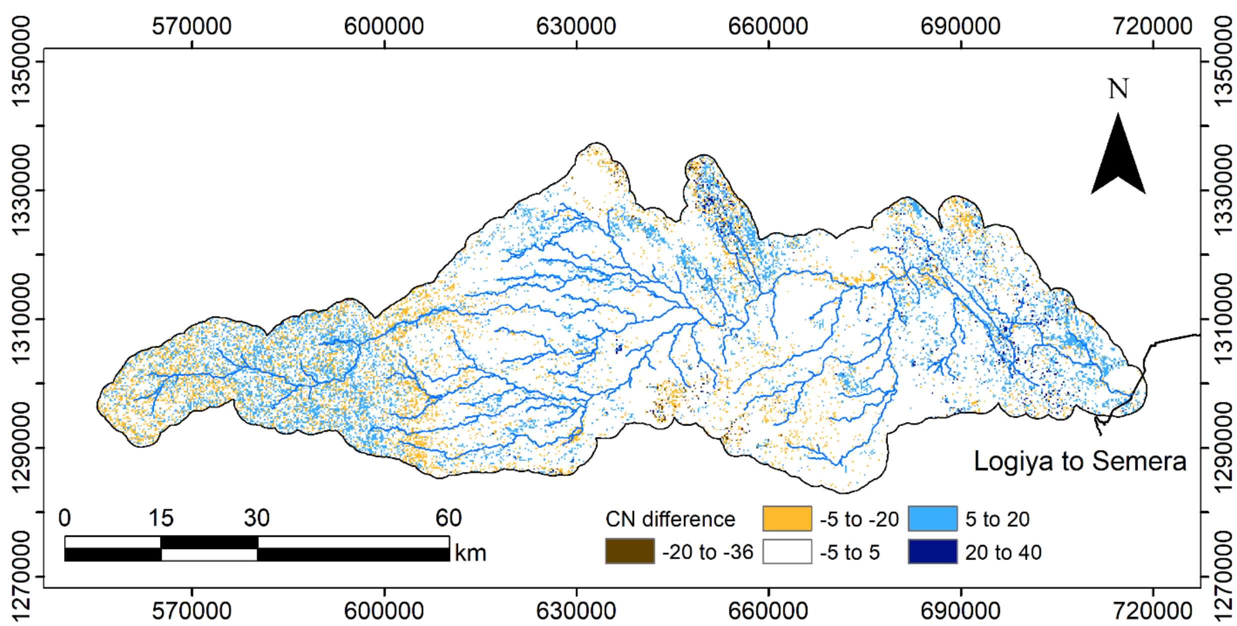


Figure 4. The difference in CN of the Logiya Catchment between 2017 and 2023

Most parts (81.22 %) of the catchment had insignificant CN differences (-5 to 5), from 2017 to 2023 (Table 2). The CN differences were positive only for about 10% of the catchment. However, these positive differences occurred near the catchment outlet and over steep topography that led to increased runoff-generating potential of the Logiya Catchment. This was in agreement with observations of the community in Logiya and Dubti towns.

Table 2. Area coverage of the Logiya Catchment under different categories of CN difference between 2017 and 2023

| Curve number difference | Percent of coverage (%) |
|---|---|
| -20 to -36 | 0.28 |
| -20 to -5 | 7.34 |
| -5 to 5 | 81.22 |
| 5 to 20 | 10.55 |
| 20 to 36 | 0.60 |

### 4.3. Flood Interaction with Infrastructure in Dubti

From 2017 to 2019, the flood caused by Logiya River was not hydraulically connected to the flood caused by Awash River, Box 1 Figure (5a). This matches with what the locals told us during the field visit. From 2017 to 2019, the flood did not affect Dubti town which was protected by the road that was constructed parallel to the main irrigation canal (CR1) (Box 2). Boxes 3 and 4 showed areas not affected by flood. The irrigated land and road (solid red dot) were not damaged by floods from 2017 to 2019.

Extreme flood in Awash Basin, particularly in Dubti, was reported in 2020. The flood washed away and damaged the roads and canals constructed for the Tendaho Irrigation Development project figure (5b). The Awash River and the flood-prone areas were connected during the 2020 extreme event, Box 1. The irrigation canal conveyed flood water (Box 1) toward Dubti town but then breached and washed away the roads and canals (CR3 and CR4). This created a new flood-prone area to increase the flood impact toward Box 4.

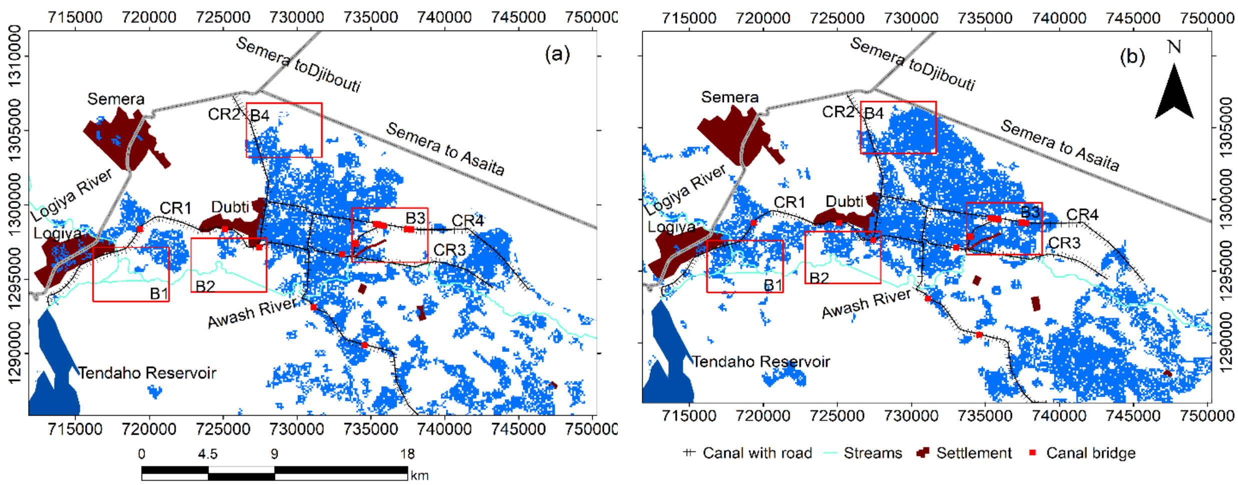


Figure 5. The flood map detected from 2017 to 2019 (a) and 2020 (b), at the flood-prone area of Dubti site and its surrounding sites

## 4.4. Flood Impact on Land Use and Land Cover Change

Table 3 showed the land cover classification accuracy of flood-prone area before post-processing. The accuracy was 73 % which was smaller than the minimum accuracy requirement, 85% (Rwanga & Ndambuki 2017). The user's and producer's accuracy were also low and varied from 62 to 76 % and 60 to 90%, respectively. The lowest accuracy was obtained for bare land, shrub, and irrigated lands. Some of the irrigated lands were correctly classified as shrub land and bare land which were, however, misclassified as irrigated land.

Table 3. The Confusion Matrix of the 2023 Land Cover Map, before Post-processing

| | Reference data | | | | | |
|---|---|---|---|---|---|---|
| LC type | Shrubland | Irrigate | Built-up | Bareland | Total | User's accuracy |
| Shrub | 15 | 5 | 0 | 4 | 24 | 62.5 |
| Irrigate | 5 | 25 | 0 | 5 | 35 | 71.4 |
| Built-up | 2 | 1 | 26 | 3 | 32 | 76.5 |
| Bareland | 3 | 1 | 3 | 23 | 30 | 71.9 |
| Total | 25 | 32 | 29 | 35 | | |
| Producer's accuracy | 60.0 | 78.1 | 89.7 | 65.7 | | Overall accuracy 73.6 |

The overall accuracy of the 2023 land cover map after post processing showed increment of 85.12 % by reducing the omission errors reported in the built-up and shrub lands (Table 4). The user's and producer's accuracy enhanced from 79 to 87.5 % and from 76 to 93.33 % respectively. The bare land with gravel introduced a commission error in the irrigated and shrub lands, while the sand was detected as a built-up to reduce the user's and producer's accuracy. The overall accuracy reported in this study substantially improved after post-processing and indicated that the land cover map could be used for evaluating the impact of floods and vice versa.

Table 4. The Confusion Matrix of the 2023 Land Cover Map, after Post-processing

| | Reference data | | | | | |
|---|---|---|---|---|---|---|
| LC type | Shrub land | Irrigate | Built-up | Bare land | Total | Users accuracy |
| Shrub | 19 | 3 | 0 | 2 | 24 | 79.2 |
| Irrigate | 3 | 30 | 0 | 2 | 35 | 85.7 |
| Built-up | 1 | 1 | 28 | 2 | 32 | 87.5 |
| Bare land | 2 | 0 | 2 | 26 | 30 | 86.7 |
| Total | 25 | 34 | 30 | 32 | | |
| Producer's accuracy | 76.00 | 88.24 | 93.33 | 81.25 | | Overall accuracy 85.12 |

The flood impact was not limited to damaging irrigated canals and roads, but it also affected the irrigated land. Figure 6 (a) and (b) showed the 2017 and 2023 land cover at the flood-prone site of lower Awash Basin, Dubti. The irrigated land of the Tendaho Irrigation Development Project was abandoned and converted to shrub land in the 2023 LC map because of the 2020 flood impact. In 2023, the built-up area in the surroundings of Dubti, Logiya, and Semera towns expanded to alter the local flood characteristics (informal communication with the Dubti town community during field observation).

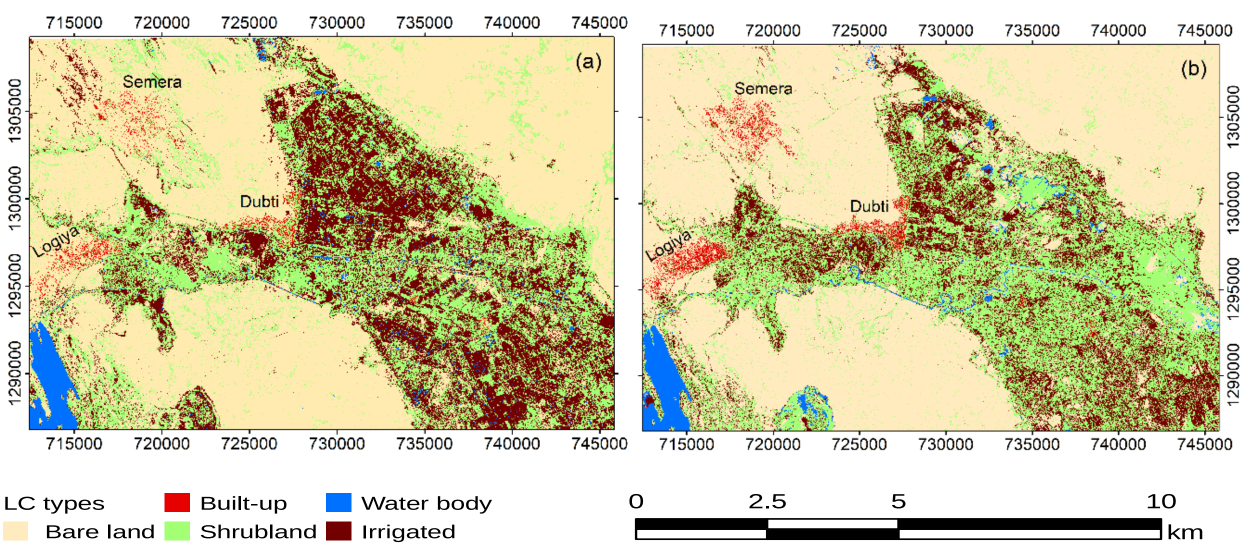


Figure 6. The 2017 and 2023 land cover maps of flood prone area shown in (a) and (b) respectively

The bare land and shrub land dominantly covered the surrounding of Dubti town. The shrub land expanded because of the 2020 flood at the expense of the bareland and irrigated land (Table 5).

Table 5. Land Cover Classes in 2017 and 2023, at Dubti town and its surroundings

| | Area coverage percentage | |
|---|---|---|
| LULC type detected | 2017 (%) | 2023 (%) |
| Bare land | 57.25 | 59.36 |
| Built-up | 0.56 | 0.85 |
| Shrub land | 21.49 | 24.65 |
| Water body | 2.08 | 2.02 |
| Irrigated land | 18.62 | 13.13 |

## 4.5. Discussion

The flooding in the lower Awash Basin was often associated with overtopping of the main Awash River with limited focus on the contribution of the tributaries. In this study, remote sensing data helped to study past floods and the contribution of the Logiya River. The remote sensing-based analysis was supported by field survey and community consultation from 2017 to 2023. Edamo et al (2022) emphasized that lack of community participation might limit flood risk management effectiveness.

Flooding was a major natural disaster that often displaced many people, but lack of ground-based data had hidden its historical characteristics and scientific evidence to manage and provide adaptation for future flood risk events. Satellites monitored the land surface at relatively short time interval to detect changes in the feature owing to flooding. The S-1 SAR operated over the land surface at day-night and any weather condition, while the S-2 optical image was suitable to assess the land cover and land use features.

Field observation and consultation with the local community allowed to fill the information gap that couldn’t be provided by remote sensing images (e.g. the flood interaction with infrastructure) and identify factor contribution for flooding. However, flood index accuracy could be affected by how threshold values were determined, i.e., either globally or locally to detect flooded pixels.  The S-1 SAR polarization affected the accuracy of the flood map (Bekele et al. 2022). Therefore, flood maps generated by VH and VV polarization were compared using ground truth data.

The findings of this study suggested that the positive CN region of Logiya Catchment could be treated by nature based solution e.g. tree planting to reduce the runoff generation potential and flood effects on Dubti. Negash et al (2023) demonstrated that expansion of built-up and agricultural area upstream of a catchment enhanced flood generation potential. The current study showed that enhanced changes in land cover were observed on steep slopes and near the catchment outlet and could have significant effects on flood generation to affect the downstream people and property.

So far, most previous studies focused on how floods impacted various land cover and land use classes (Zope et al., 2016). However, this study indicated that the infrastructure (roads and canals) influenced the spatial pattern of floods and associated impacts. Therefore, the planning, design, and construction of infrastructures should be based on water sensitivity and flood studies. For example, some infrastructures generated false sense of water security regarding flood protection (observed in field observation along the flood-plain of upper and lower Awash Basin). Around Dubti site, the main irrigation canal constructed by Tendaho Irrigation Development project conveyed the Logiya River overflows toward Dubti town and over the irrigated land during the extreme floods in 2020. This agreed with Njogu's (2021) research findings that the infrastructure development over flood-plains affected the flood characteristics. It suggested the need to consider the implications of infrastructures on flooding during the design and construction stages (Taye et al. 2024). Bekele et al (2022) showed that the Addis Ababa to Adama road and flood wall constructed by community intervened with the natural flow direction, contributing to the flooding in Akaki Catchment.

The findings of this study could be enhanced through additional ground control points and the use of rainfall-runoff models. However, modeling applications were constrained by stream-flow data availability. Citizen science provided an opportunity to engage the public in generation of stream-flow data and hydrological knowledge generation. However, there were only limited studies that applied citizen science for flood studies.

## 5. Conclusions and Recommendations

In this study, the Sentinel-1 SAR and Sentinel-2 optical satellite images were used for historical flood and land cover change monitoring, respectively. The following conclusions were drawn based on the results of this study:-

- The accuracy of land cover classification using CART could be enhanced using remote sensing indices for post-processing.
- The remote sensing approach enabled the examination of the infrastructure impact on flood characteristics. Considering the rapid development of infrastructures in Ethiopia, potential interactions between infrastructures and floods needed to be investigated prior to infrastructure development.
- High temporal revisit (6 days) of S-1 SAR images over the Dubti flood-prone area allowed reasonable representation of the spatial and temporal variability of flood characteristics.
- Community consultation provided actual ground truth data to evaluate historical flood and fill the remote sensing gap. In detecting the flood interaction with infrastructure (road and irrigation canal) constructed at the flood-prone area.
- Multi-causality of extreme flood events was identified in this study but it required further investigation across various flood prone areas.

**Acknowledgement**

This article was an output from the REACH Programme, funded by UK Aid from the UK Foreign, Commonwealth and Development Office (FCDO) for the benefit of developing countries (Programme Code 201880).

**Data availability**

Data will be available on request.

**References**

Alemu, A. N., Haile, A. T., Carr, A. B., Trigg, M. A., Mengistie, G. K., & Walsh, C. L. (2023). Filling data gaps using citizen science for flood modeling in urbanized catchment of akaki. Natural Hazard Research. https://doi.org/10.1016/j.nhres.2023.05.002

Anusha, N., & Bharathi, B. (2020). Flood detection and flood mapping using multi-temporal synthetic aperture radar and optical data. Egyptian Journal of Remote Sensing and Space Science, 23(2), 207–219. https://doi.org/10.1016/j.ejrs.2019.01.001

Asfaw, W., Rientjes, T., Bekele, T. W., & Haile, A. T. (2025). Estimating elements susceptible to urban flooding using multisource data and machine learning. International Journal of Disaster Risk Reduction, 116(December 2024), 105169. https://doi.org/10.1016/j.ijdrr.2024.105169

Bekele, T. W., Haile, A. T., Trigg, M. A., & Walsh, C. L. (2022). Evaluating a new method of remote sensing for flood mapping in the urban and peri-urban areas: Applied to Addis Ababa and the Akaki catchment in Ethiopia. Natural Hazards Research, February. https://doi.org/10.1016/j.nhres.2022.03.001

Bibi, T. S., Kara, K. G., Bedada, H. J., & Bededa, R. D. (2023). Application of PCSWMM for assessing the impacts of urbanization and climate changes on the efficiency of stormwater drainage systems in managing urban flooding in Robe town, Ethiopia. Journal of Hydrology: Regional Studies, 45(September 2022), 101291. https://doi.org/10.1016/j.ejrh.2022.101291

Cao, H., Zhang, H., Wang, C., & Zhang, B. (2019). Operational flood detection using Sentinel-1 SAR data over large areas. Water (Switzerland), 11(4). https://doi.org/10.3390/w11040786

Carr, A. B., Trigg, M. A., Haile, A. T., Bernhofen, M. V., Alemu, A. N., Bekele, T. W., & Walsh, C. L. (2024). Using global datasets to estimate flood exposure at the city scale: an evaluation in Addis Ababa. Frontiers in Environmental Science, 12(February), 1–14. https://doi.org/10.3389/fenvs.2024.1330295

Clement, M., Kilsby, C., & Moore, P. (2017). Multi-Temporal SAR Flood Mapping using Change Detection Multi-temporal synthetic aperture radar fl ood mapping using change detection. April. https://doi.org/10.1111/jfr3.12303

Dash, P., Sanders, S. L., Parajuli, P., & Ouyang, Y. (2023). Improving the Accuracy of Land Use and Land Cover Classification of Landsat Data in an Agricultural Watershed. Remote Sensing, 15(16), 1–24. https://doi.org/10.3390/rs15164020

Edamo, M. L., Ukumo, T. Y., Lohani, T. K., Ayana, M. T., Ayele, M. A., Mada, Z. M., & Abdi, D. M. (2022). A comparative assessment of multi-criteria decision-making analysis and machine learning methods for flood susceptibility mapping and socio-economic impacts on flood risk in Abela-Abaya floodplain of Ethiopia. Environmental Challenges, 9(July). https://doi.org/10.1016/j.envc.2022.100629

Erena, S. H., & Worku, H. (2019). Urban flood vulnerability assessments: the case of Dire Dawa city, Ethiopia. Natural Hazards, 97(2), 495–516. https://doi.org/10.1007/s11069-019-03654-9

Fang, R., Hon, J., Zhou, M., & Lu, Y. (2022). An Empirical Energy Landscape Reveals

Mechanism of Proteasome in Polypeptide Translocation. ELife, 11, 1–28. https://doi.org/10.7554/eLife.71911

Gorelick, N., Hancher, M., Dixon, M., Ilyushchenko, S., Thau, D., & Moore, R. (2017). Google Earth Engine: Planetary-scale geospatial analysis for everyone. Remote Sensing of Environment, 202, 18–27. https://doi.org/10.1016/j.rse.2017.06.031

Haile, A. T., Asfaw, W., Rientjes, T., & Worako, A. W. (2022). Deterioration of streamflow monitoring in Omo-Gibe basin in Ethiopia. Hydrological Sciences Journal, 67(7), 1040–1053. https://doi.org/10.1080/02626667.2022.2060110

Haile, A. T., Bekele, T. W., Derso, E., Mekuria, W., & Ruckstuhl, S. (2024). Urgent flood hazard assessment using multi-sensor data in refugee hosting community settings : Implications for immediate planning and design of anticipatory actions. Colombo, Sri Lanka: International Water Management Institute (IWMI). CGIAR Initiative on Fragility, Conflict, and Migration. 10p.

Haile, A. T., Bekele, T. W., & Rientjes, T. (2023). Interannual comparison of historical floods through flood detection using multi-temporal Sentinel-1 SAR images, Awash River Basin, Ethiopia. International Journal of Applied Earth Observation and Geoinformation, 124(June), 103505. https://doi.org/10.1016/j.jag.2023.103505

Kianfar, N. (2019). The applicability of dual polarized sentinel-1 sar data for detection of flooded areas in pol-e dokhtar , lorestan , iran. Xlii(october), 12–14. https://doi.org/10.5194/isprs-archives-XLII-4-W18-655-2019

Leta, B. M., & Adugna, D. (2023). Characterizing the level of urban Flood vulnerability using the social-ecological-technological systems framework, the case of Adama city, Ethiopia. Heliyon, 9(10), e20723. https://doi.org/10.1016/j.heliyon.2023.e20723

Li, Y., Martinis, S., Plank, S., & Ludwig, R. (2018). An automatic change detection approach for rapid fl ood mapping in Sentinel-1 SAR data. Int J Appl Earth Obs Geoinformation. 73(March), 123–135. https://doi.org/10.1016/j.jag.2018.05.023

Malede, D. A., Andualem, T. G., Yibeltal, M., Alamirew, T., kassie, A. E., Demeke, G. G., & Mekonnen, Y. G. (2024). Climate change impacts on hydroclimatic variables over Awash basin, Ethiopia: a systematic review. Discover Applied Sciences, 6(1). https://doi.org/10.1007/s42452-024-05640-8

Manandhar, R., Odehi, I. O. A., & Ancevt, T. (2009). Improving the accuracy of land use and land cover classification of landsat data using post-classification enhancement. Remote Sensing, 1(3), 330–344. https://doi.org/10.3390/rs1030330

Matheswaran, K., Alahacoon, N., Pandey, R., & Amarnath, G. (2019). Flood risk assessment in South Asia to prioritize flood index insurance applications in Bihar, India. Geomatics, Natural Hazards and Risk, 10(1), 26–48. https://doi.org/10.1080/19475705.2018.1500495

Miller, J. D., Kim, H., Kjeldsen, T. R., Packman, J., Grebby, S., & Dearden, R. (2014). Assessing the impact of urbanization on storm runoff in a peri-urban catchment using historical change in impervious cover. Journal of Hydrology, 515, 59–70. https://doi.org/10.1016/j.jhydrol.2014.04.011

Mohammadi, A., Khalil Valizadeh Kamran, Sadra Karimzadeh, Shahabi, H., & Nadhir Al-Ansari 6. (2020). Complexity - 2020 - Mohammadi - Flood Detection and Susceptibility Mapping Using Sentinel-1 Time Series Alternating. https://doi.org/10.1155/2020/4271376

Munasinghe, D., Frasson, R. P. de M., David, C. H., Bonnema, M., Schumann, G., & Brakenridge, G. R. (2023). A multi-sensor approach for increased measurements of floods and their societal impacts from space. Communications Earth and Environment, 4(1), 1–10. https://doi.org/10.1038/s43247-023-01129-1

Negash, E. D., Asfaw, W., Walsh, C. L., Mengistie, G. K., & Haile, A. T. (2023). Effects of land use land cover change on streamflow of Akaki. Sustainable Water Resources Management, 4. https://doi.org/10.1007/s40899-023-00831-4

Njogu, H. W. (2021). Effects of floods on infrastructure users in Kenya. Journal of Flood Risk Management, 14(4), 1–10. https://doi.org/10.1111/jfr3.12746

Nuthammachot, N., Phairuang, W., & Stratoulias, D. (2017). Removing speckle noise in Sentinel-1A radar satellite imagery using filtering techniques. February, 0–14. https://www.researchgate.net/publication/313845253

Prabhu, N., Mohan Kumar, T. M., & Inayathulla, M. (2020). Runoff estimation for Arkavathi valley, hebbala valley, KC Valley, South Pennar valley, Vrishabhavathi valley by using soil conservation services curve number method (Scs-cn). Water and Energy International, 63r(2), 57–66. https://www.researchgate.net/publication/341941141

Rwanga, S. S., & Ndambuki, J. M. (2017). Accuracy Assessment of Land Use/Land Cover Classification Using Remote Sensing and GIS. International Journal of Geosciences, 08(04), 611–622. https://doi.org/10.4236/ijg.2017.84033

Tamiru, H., & Dinka, M. O. (2021). Application of ANN and HEC-RAS model for flood inundation mapping in lower Baro Akobo River Basin, Ethiopia. Journal of Hydrology: Regional Studies, 36, 100855. https://doi.org/10.1016/j.ejrh.2021.100855

Taye, M. T., Dyer, E., Hirpa, F. A., & Charles, K. (2018). Climate change impact on water resources in the Awash basin, Ethiopia. Water (Switzerland), 10(11), 1–16. https://doi.org/10.3390/w10111560

Taye, M. T., Nicol, A., & Dyer, E. (2024). Policy and practice recommendations on flood risk management in the Awash basin. REACH Discussion brief.

Thakkar, A. K., Desai, V. R., Patel, A., & Potdar, M. B. (2017). Post-classification corrections in improving the classification of Land Use/Land Cover of arid region using RS and GIS: The case of Arjuni watershed, Gujarat, India. Egyptian Journal of Remote Sensing and Space Science, 20(1), 79–89. https://doi.org/10.1016/j.ejrs.2016.11.006

Zeng, Z., Gan, Y., Kettner, A. J., Yang, Q., Zeng, C., Brakenridge, G. R., & Hong, Y. (2020). Towards high resolution flood monitoring: An integrated methodology using passive microwave brightness temperatures and Sentinel synthetic aperture radar imagery. Journal of Hydrology, 582, 124377. https://doi.org/10.1016/j.jhydrol.2019.124377